Cell, Volume *135*

Supplemental Data

Nf1-Dependent Tumors Require a Microenvironment Containing *Nf1*$^{+/-}$- and c-kit-Dependent Bone Marrow

Feng-Chun Yang, David A. Ingram, Shi Chen, Yuan Zhu, Jin Yuan, Xiaohong Li, Xianlin Yang, Scott Knowles, Whitney Horn, Yan Li, Shaobo Zhang, Yanzhu Yang, Saeed T. Vakili, Menggang Yu, Dennis Burns, Kent Robertson, Gary Hutchins, Luis F. Parada, and D. Wade Clapp

Supplemental Figure 1

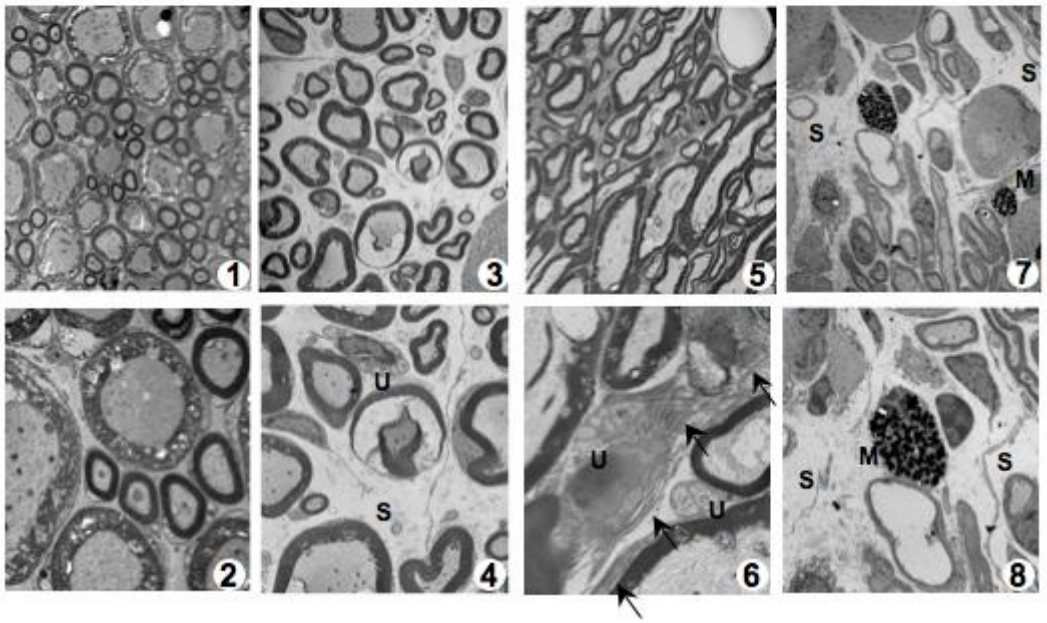

Figure S1. Ultrastructural Analysis of Dorsal Root Ganglia by Transmission Electron Microscopy

Panels 1-4, 750 X, panels 5-8, 1500 X. Panel 1-2 proximal spinal nerves from a *Krox20;Nf1*$^{flox/flox}$ mouse transplanted with WT BM; Panels 3-8 proximal nerves from recipients transplanted with *Nf1*+/- BM. (U) unmyelinated axons; (S) indicates expansion of the endoneurial space. Arrowheads identify collagen bundles. (M) indicates mast cells infiltrating the tumor.

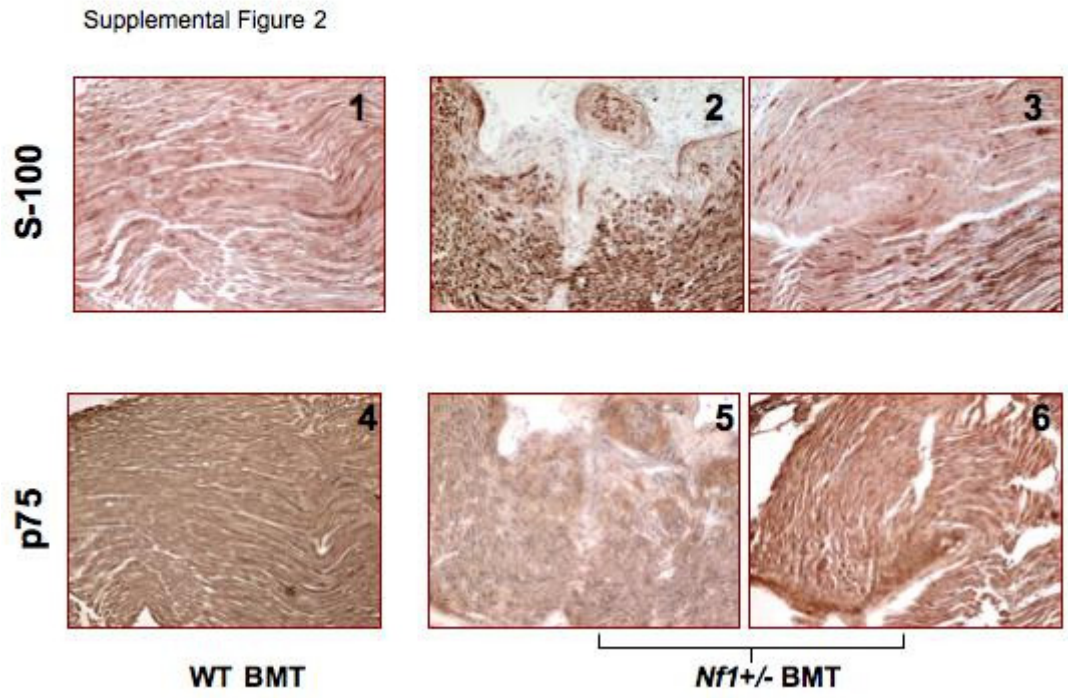

Figure S2. Immunohistochemical Analysis of Neurofibromas in Sciatic Nerves

Sciatic nerves from *Krox20;Nf1*$^{flox/flox}$ recipient mice 10 months following transplantation. Nerves were sectioned and stained with anti-S100 and anti-p75^{NGFR} antibodies. Tumors contained both S100 and p75NGFR expression though there is cell to cell variability consistent with the heterogeneous nature of the tumors observed in previous studies (Zhu et al., 2002). All photomicrographs are 200X. The genotypes of donor bone marrow cells and the antibodies utilized for staining are indicated.

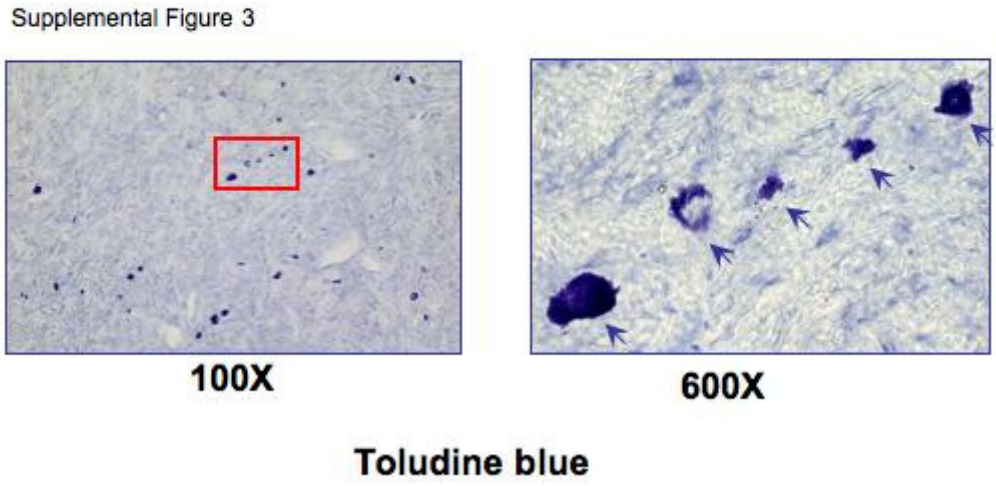

Figure S3. Identification of Mast Cells within Tumors Using Histochemical Staining

Tumors were stained with toluidine blue to identify mast cells within tumors. A 100 X and 600 X magnification of an inset (shown in red) from a tumor identify mast cells which stain deep blue-purple. The data are similar to data in Figure 3C-D.

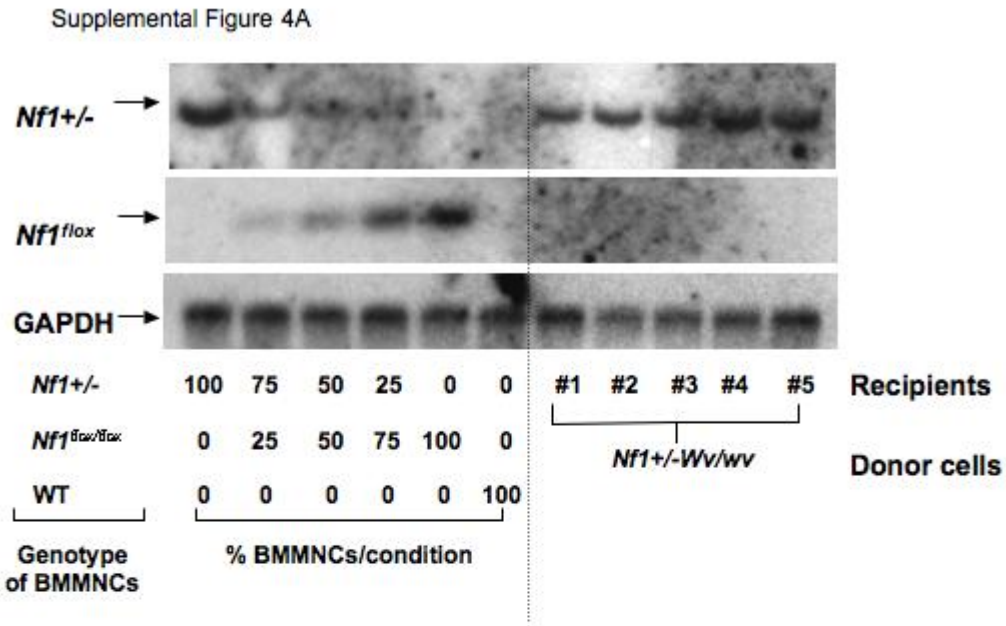

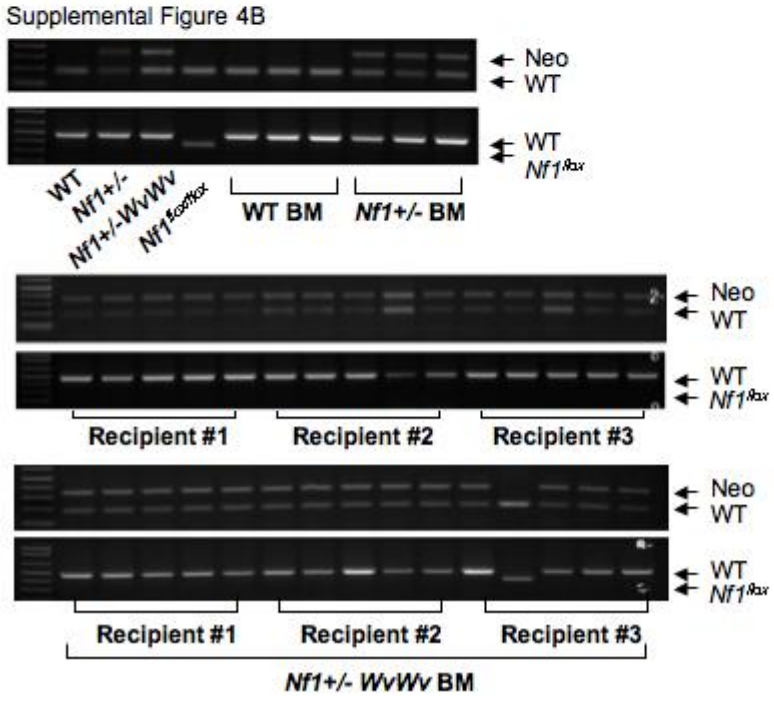

Figure S4. Genotypic Identification of DNA from Bone Marrow of Irradiated *Krox20;Nf1*$^{flox/flox}$ Recipients Transplanted with *Nf1+/-; Wv/Wv* Bone Marrow

A. Evaluation of mature progeny by Southern blot**.** Ten micrograms of DNA from recipient bone marrow was isolated, digested with a restriction endonuclease that cleaves both the *Nf1* knockout and the *Krox20;Nf1*$^{flox/flox}$ alleles and allows determination of the relative intensity of each allele following Southern blot analysis. Equivalent amounts of DNA isolated from a range of mixtures of *Nf1*+/- and *Nf1*$^{flox/flox}$ bone marrow cells were analyzed on the same blot to allow quantitative analysis of the respective alleles. The ratios of DNA from control cells, the identity of the respective alleles, relative DNA loading and recipient samples are indicated. Recipient 1 (*85% Nf1*+/-), Recipient 2 (95% *Nf1+/-),* Recipient 3 (97% *Nf1*+/-), Recipient 4 (100% *Nf1*+/-), recipient 5 (97 % *Nf1*+/-). B. Genotypic identification of DNA from progenitors. Bone marrow from the same recipients as in A was cultured in semisolid medium to promote growth of myeloid and mast cell progenitors. DNA from individual colonies was isolated and amplified for the WT, *Nf1* null and *Nf1*$^{flox/flox}$ allele using polymerase chain reaction. Top panel. DNA from representative progenitors of the indicated genotypes was amplified in two independent reactions to identify donor and endogenous genotypes. The DNA products and genotypes are indicated. Middle Panel: Representative PCR products of DNA isolated from mast cell progenitors of 3 recipients. Bottom Panel: Representative PCR products of DNA from granulocyte-macrophage progenitors from 3 recipients. 90 CFU-Mast (18 CFU-mast/recipient) were analyzed. 110 CFU-GM progenitors (22 CFU-GM/recipient) were scored. The PCR product was found to be donor in origin in 94-100% of all progenitors isolated from each respective recipient.

Supplemental Figure 5A

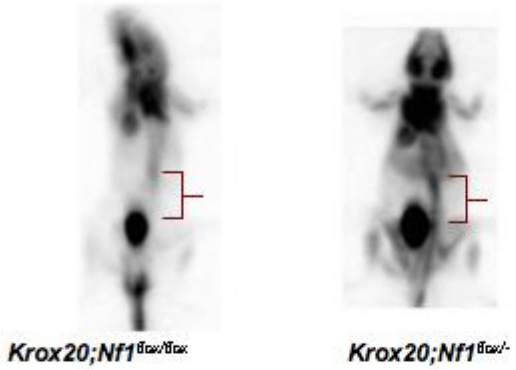

Supplemental Figure 5B

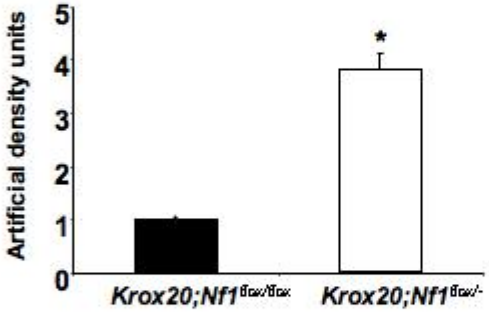

Supplemental Figure 5C

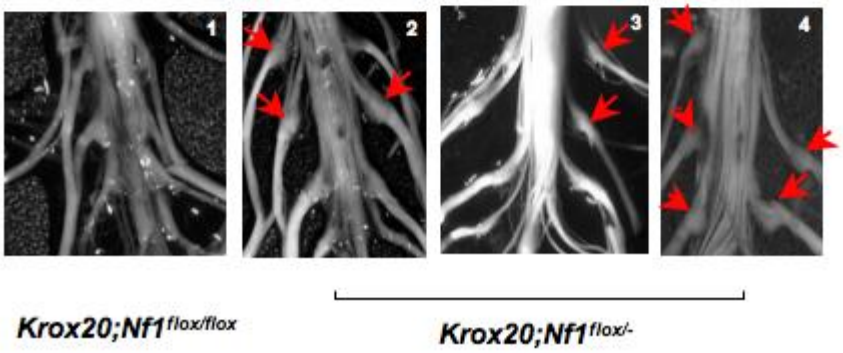

Figure S5. Identification of Plexiform Neurofibromas Using FDG-PET

A. FDG-PET images and dissection of spinal nerves of a *Krox20;Nf1*$^{flox/flox}$ mouse and *Krox20;Nf1*$^{flox/-}$ mouse imaged at 9 months of age. B. Mean intensity of FDG-PET from the sciatic nerve region of interests in *Krox20;Nf1*$^{flox/-}$ and

Krox20;Nf1$^{flox/flox}$ mice. C. Representative dissections from the dorsal root ganglia from a *Krox20;Nf1*$^{flox/flox}$ mouse (Panel 1) and *Krox20;Nf1*$^{flox/-}$ mice with PET positive tumors (Panels 2-4).

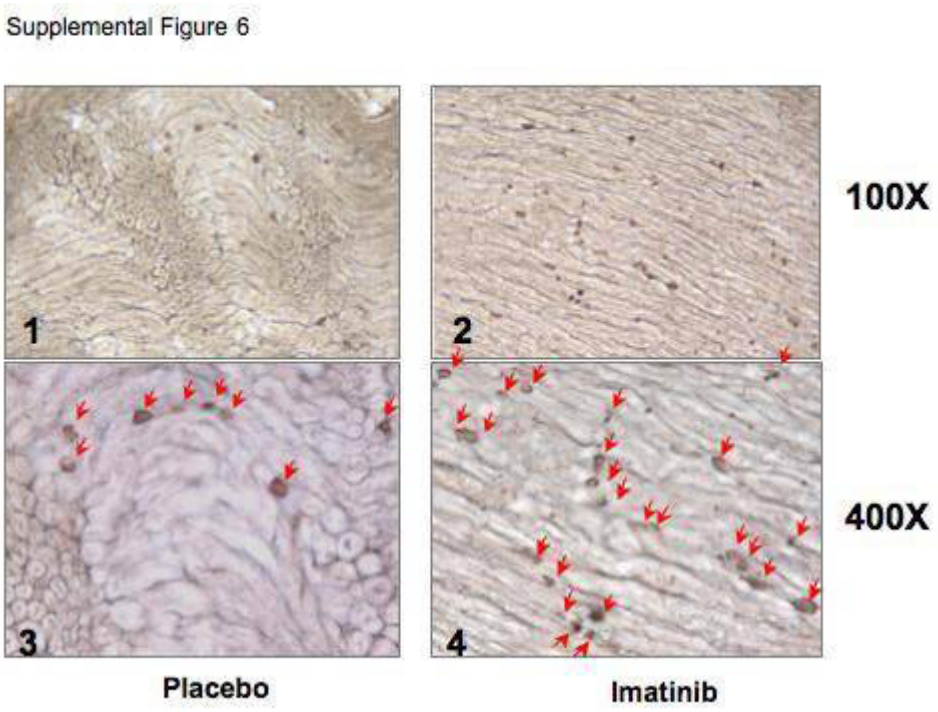

Figure S6. Evaluation of Apoptosis in Plexiform Neurofibromas Using TUNEL Following Treatment with Imatinib Mesylate or Placebo

Representative sections from plexiform neurofibromas treated with a placebo control (left panel) or imatinib mesylate (right panel). Arrowheads indicate TUNEL positive cells.

Supplemental Figure 7

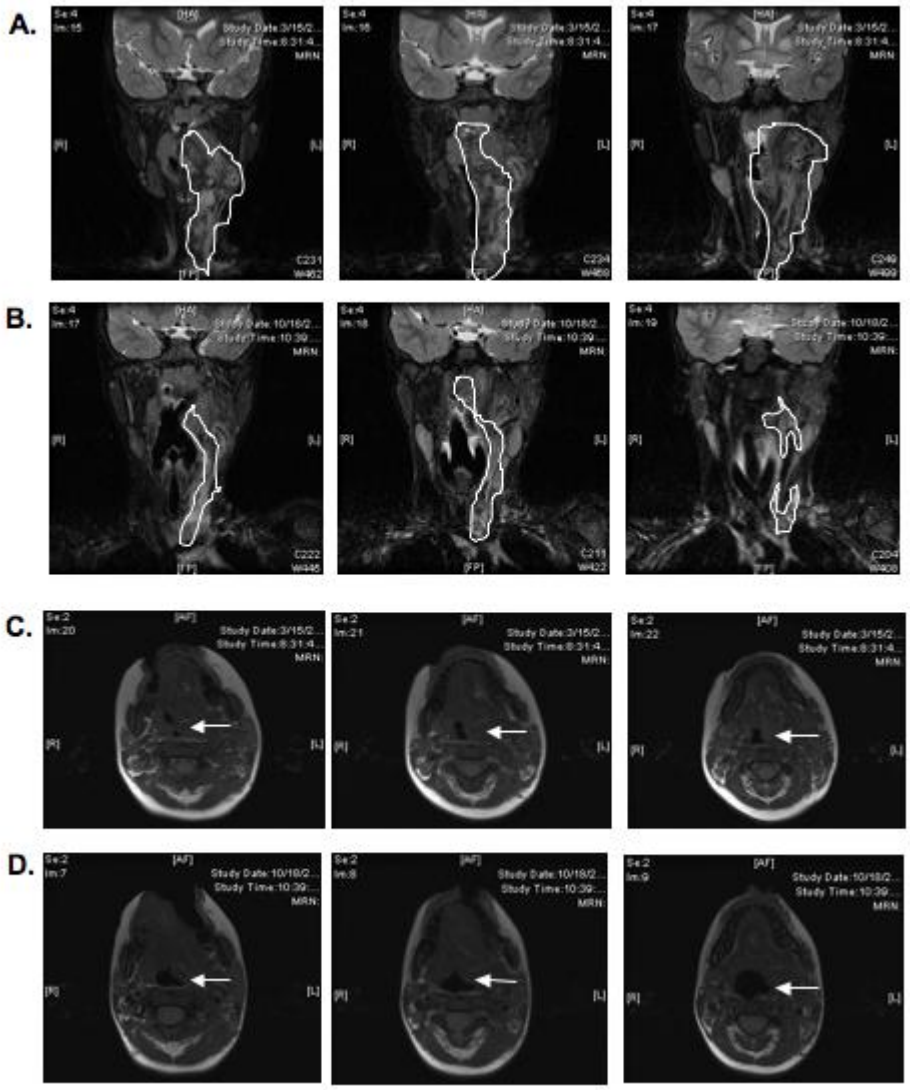

Figure S7. MRI Images, Head and Neck

A, B: Coronal MRI T1 weighted STIR sequence images; pre-imatinib-mesylate and 6 months following treatment with imatinib mesylate, respectively. C, D: Axial MRI T2 weighted sequence images; before and after 6 months of treatment with imatinib mesylate respectively. On both series of images, note marked narrowing of the upper airway (arrow) with displacement to the right by tumor in the pre-imatinib mesylate images. Post-imatinib mesylate, there is marked improvement with airway enlargement back toward the midline. The regions of the tumor in the respective images are indicated.

Table S1.

Phenotype of *Krox20;Nf1*$^{flox/flox}$ after bone marrow transplantation of BMMNCs

Genotype of BM cells	Experimental Mice count	Phenotype of mice	Morbidity (%)
WT	22	Enlarged dorsal root ganglia (0/22)	0
		Plexiform neurofibromas (0/22)	0
		Motor abnormality (0/22)	0
		Atonic bladder (0/22)	0
		Hydronephrosis (0/22)	0
Nf1+/-	22	Enlarged dorsal root ganglia (21/22)	95
		Plexiform neurofibromas (21/22)	95
		Motor abnormality (6/22)	27
		Atonic bladder / Hydronephrosis (5/22)	23